A Journal of the Gesellschaft Deutscher Chemiker
Angewandte Chemie
International Edition
GDCh
www.angewandte.org

Accepted Article

Title: Structural Engineering of Luminogens with High Emission Efficiency both in Solution and the Solid State

Authors: Yanli Zhao, Hongwei Wu, Zhao Chen, Weijie Chi, Bindra Anivind Kaur, Long Gu, Cheng Qian, Bing Wu, Bingbing Yue, Guofeng Liu, Guangbao Yang, and Liangliang Zhu

To be cited as: *Angew. Chem. Int. Ed.* 10.1002/anie.201906507
Angew. Chem. 10.1002/ange.201906507

Link to VoR: http://dx.doi.org/10.1002/anie.201906507
http://dx.doi.org/10.1002/ange.201906507

WILEY-VCH

10.1002/anie.201906507

Structural Engineering of Luminogens with High Emission Efficiency both in Solution and the Solid State

Hongwei Wu, Zhao Chen, Weijie Chi, Bindra Anivind Kaur, Long Gu, Cheng Qian, Bing Wu, Bingbing Yue, Guofeng Liu, Guangbao Yang, Liangliang Zhu* and Yanli Zhao*

Abstract: *Developing molecules with high emission efficiency both in solution and the solid state is still a great challenge, since most organic luminogens are either aggregation-caused quenching or aggregation-induced emission molecules. We overcame this dilemma via integrating planar and distorted structures with long alkyl side chains to achieve DAπAD type emitters. Linear diphenyl-diacetylene core and charge transfer effect ensure considerable planarity of these molecules in excited state, allowing strong emission in dilute solution (quantum yield up to 98.2 %). On the other hand, intermolecular interactions of two distorted cyanostilbene units restrict molecular vibration and rotation, and long alkyl chains reduce the quenching effect of the π-π stacking to the excimer, eventually leading to strong emission in the solid state (quantum yield up to 60.7 %). Thus, multiple bioimaging upon varying the concentration of the emitters was well established, which may provide a new vision for applying bright luminescent materials in a variety of environments.*

Organic luminescent materials have been applied in numerous areas such as bioimaging,[1-3] drug release,[4,5] sensors,[6] light-emitting diodes,[7-10] and memory devices.[11] Most of the luminogens suffer from aggregation-caused quenching (ACQ), where they can only emit strongly in dilute solution while showing weak or even no emission in aggregated or solid state.[12] In addition, another type of molecules, namely aggregation induced emission (AIE) molecules[13-15] could exhibit non-radiative decay *via* intramolecular rotation in dilute solution whereas becoming highly emissive in aggregated or solid state. Nevertheless, obtaining luminophores that can emit strongly both in dilute solution and the solid state is still a great challenge. Tang and coworkers applied the conjugation-induced rigidity effect to obtain three triphenylamine fluorophores showing strong emission in single molecular and aggregated states.[16] Huang *et al.* developed self-assembled cages containing Pt(II) centers and tetraphenylethylene ligands to produce strong emission in both dilute solution and aggregated state.[17] In these cases, specific stereogeometry and distinct photophysical properties between amorphous and aggregated crystalline states were required. A concise but more precise molecular design for fabricating such dual-phase (solution and solid state) highly emissive luminophores is desired.

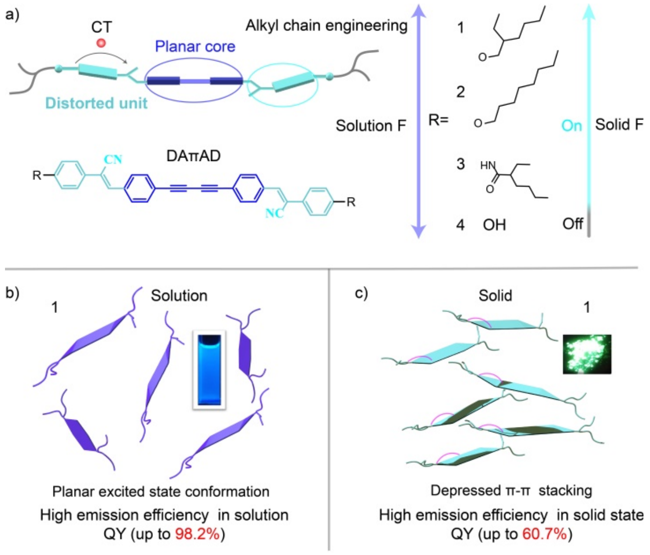

Figure 1. Illustration of combined structural engineering (planar core + distorted unit + alkyl side chain) for the design of linear DAπAD type emitters. a) Chemical structures of compounds **1**-**4**. F represents fluorescence. b) Schematic representation of a planar excited state of compound **1**, leading to strong emission in solution. c) Schematic representation of a proposed molecular alignment of compound **1**, where the distorted CS unit limits intramolecular vibration and rotation, and long alkyl chain depresses unfavorable face-to-face π-π stacking interaction, leading to strong emission in the solid state. Insets in b,c) show bright photoluminescence of compound **1** in dilute solution and solid powder state, respectively.

Inspired by these relevant findings where the gap between ACQ and AIE compounds can be eliminated by structural engineering, herein, we present a rational strategy to create luminogens with high emission efficiency both in solution and the solid state, so as to achieve advanced emissive applications. Since bright molecules in solution require substantial structural rigidity to limit intramolecular motions,[18] we here employed a planar diphenyl-diacetylene (DPDA) structure[19] as the core to constitute π-conjugated molecules (Figure 1). As compared to single and double bond skeletons, the diacetylene group can greatly limit molecular twisting and improve the regularity of the molecules by connecting with two benzene rings. On the other hand, considerable distorted conformation is also needed to prevent detrimental exciton interactions in the solid state. Therefore, we introduced donor-acceptor (D-A) type cyanostilbene (CS) to DPDA to suppress molecular rotation for improved solid-state emission. Though CS is distorted in the solid state, it may also become planar in dilute solution due to the bond length change under the charge transfer (CT) effect. Meanwhile, we added long alkyl side chains[20] to the CS unit

---

[a] Dr. H. Wu,[†] Mr. B. Wu, Ms. B. Yue, Prof. Dr. L. Zhu
State Key Laboratory of Molecular Engineering of Polymers
Department of Macromolecular Science
Fudan University, Shanghai 200438, China
E-mail: zhuliangliang@fudan.edu.cn
[b] Dr. H. Wu, Ms. B. A. Kaur, Dr. L. Gu, Dr. C. Qian, Dr. G. Liu, Dr. G. Yang, Prof. Y. L. Zhao
Division of Chemistry and Biological Chemistry
School of Physical and Mathematical Sciences
Nanyang Technological University
21 Nanyang Link, Singapore 637371
E-mail: zhaoyanli@ntu.edu.sg
[c] Dr. Z. Chen[†]
School of Computer Science and Technology
Donghua University, Shanghai 201620, China
[d] Dr. W. Chi
Singapore University of Technology and Design
8 Somapah Road, Singapore 487372

[†] These authors contributed equally to this work.

Supporting information for this article is given via a link at the end of the document.

with the anticipation of suppressing unfavorable π–π stacking interactions in the solid state to further enhance the quantum yield (QY). The alkyl chains would not affect the planarity of the molecules for showing strong emission in solution state because of their flexibility. Thus, four compounds **1**-**4** with the same DAπAD (Figure 1a) structure but different side alkyl chains were prepared for the investigations. Their synthesis is detailed in the Supporting Information.

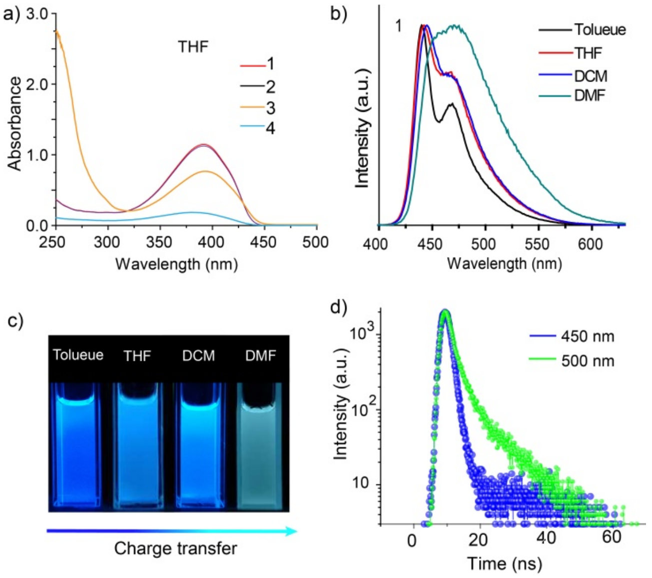

Figure 2. Photophysical properties in solution. a) Absorbance spectra of compounds **1**-**4** in THF. b) Normalized emission spectra of compound **1** in different solvents upon 365 nm excitation. c) Photographs of compound **1** in corresponding solutions under a 365 nm UV light. d) Photoluminescent lifetime of compound **1** in DMF upon 365 nm excitation measured at 450 and 500 nm emission. All measurements were performed at room temperature with the concentration of 10 μM.

Photophysical properties of these compounds were firstly investigated in different solutions. Compounds **1**-**4** all show the maximum absorption peaks at about 390 nm in tetrahydrofuran (THF, Figure 2a). Meanwhile, they present strong emission in different solvents (Figures 2b and S1). In particular, the highest peak around 440 nm and a shoulder peak around 470 nm were observed in toluene, which might be associated with two different luminescent moieties (DPDA and CS). They also exhibit similar emission bands in dichloromethane (DCM) and THF. In addition, the two peaks could merge into a single band with longer wavelength in N,N-dimethylformamide (DMF), featuring the CT effect in these molecules.[20,21] For instance, compound **1** exhibits bright emission in different solvents under the UV light (Figure 2c), and the emission color changes from blue (in THF) to green (in DMF) with the increase of the solvent polarity (Figure S2). The CT character could also be proven by the decreased absorption peak at around 400 nm, due to the increase of the dipole moment in the CT state upon increasing the solvent polarity (Figure S1d). The fluorescence lifetime increases from 1.5 ns (at 450 nm) to 3.0 ns (at 500 nm) due to the emission redshift (Figure 2d). The fluorescence QY of four compounds in THF is 98.2%, 74.7 %, 96.3%, and 39.5 %, respectively.

For further understanding the intense emission in dilute solution, we need to know the molecular conformation that dominates the emission property. As crystal structures were difficult to obtain, we employed computational study to explore the ground and excited state conformation of compounds **1** and **4**. Density functional theory (DFT) calculations show that the HOMO is located on the whole aromatic structures. However, the LUMO distribution on the methoxybenzene unit becomes lesser on account of its electron donor property (Figure 3a). Photoexcitation to the first excited singlet state (S_1) mainly involves the transition from HOMO to LUMO with large oscillator strength of 3.4292 and 3.2071 for compounds **1** and **4**, respectively. Moreover, compounds **1** (387 nm) and **4** (385 nm) show similar maximum absorption wavelength, which are in good agreement with experimental results (Figure 2a). As compared to the structures in the ground state, molecular conformation in the excited state tends to be more planar, evidenced by the rotation of dihedral angle between phenyl and cyano groups from ~25° to ~4° (Figure 3b). The CT effect between electron withdrawing cyano group and electron donating benzene ring could increase the bond length and relax the distorted conformation in the excited state. Weak emission in solution might be observed if the molecule does not have such a structure for the CT effect.[22] Since the excited state conformation largely determines the molecular emission property, such a planar conformation in the excited state could effectively diminish the molecular vibration and rotation so as to improve the efficiency of radiative process. Thus, the bright emission property of these molecules was unambiguously observed in dilute solution. In addition, compound **4** showed the lowest QY, perhaps due to weaker electronic ability of the phenolic hydroxyl group as compared to the alkoxy one on other compounds. Strong electron donating ability could promote the CT effect for molecules with more planar conformation in solution.

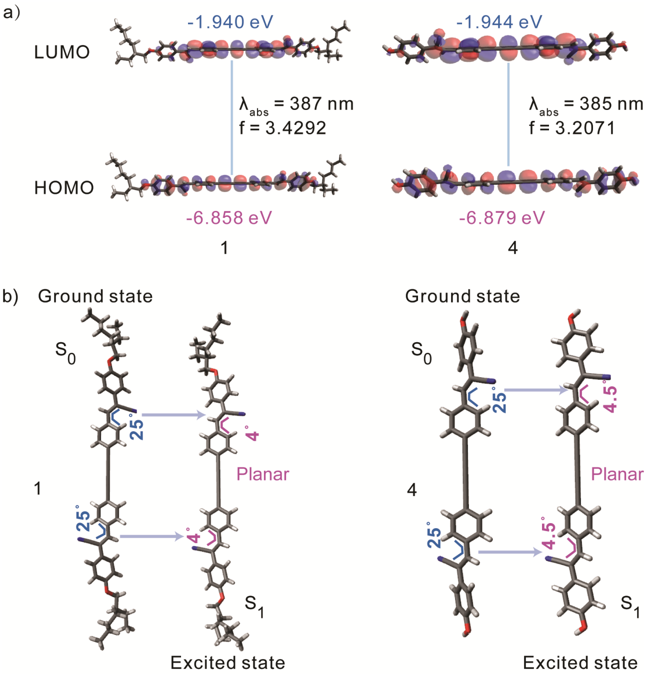

Figure 3. a) HOMO and LUMO distribution, and photoexcitation properties of compounds **1** and **4**. b) Geometrical conformation of compounds **1** and **4** in ground and excited states.

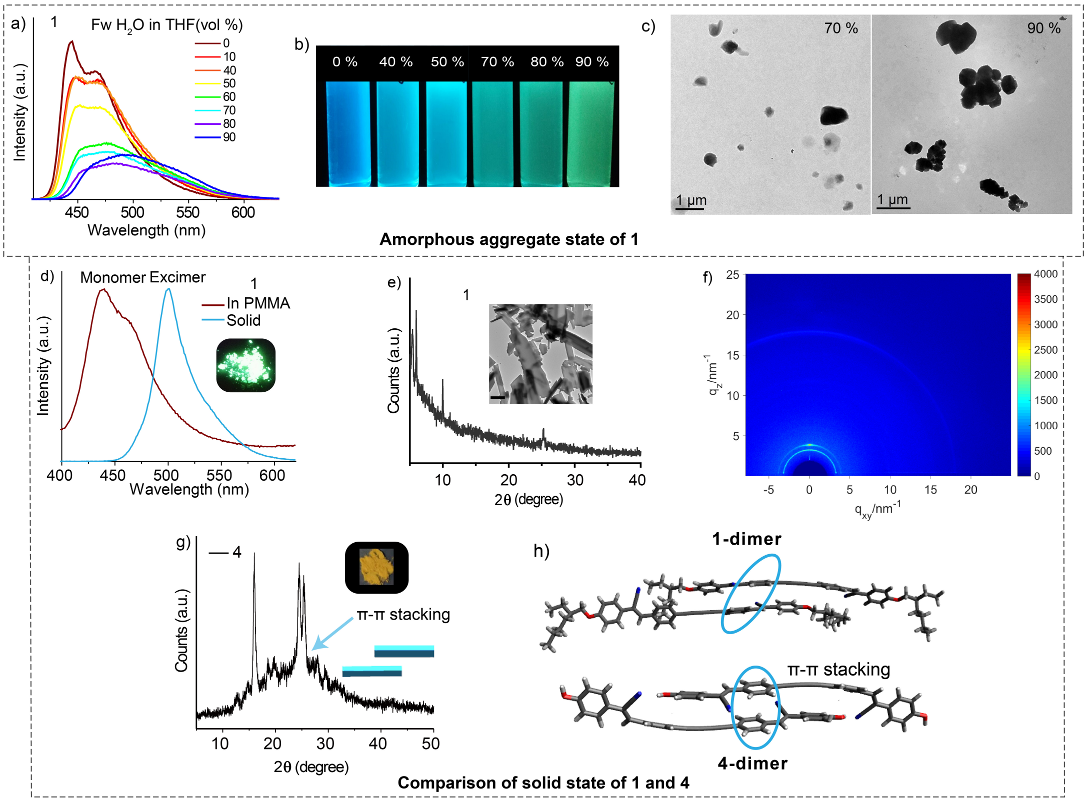

Figure 4. Photophysical studies in the solid state. a) Emission spectra of compound **1** (100 μM) in THF/H$_2$O with different water fractions under 365 nm excitation. b) Photographs of compound **1** in THF/H$_2$O with different water fractions under 365 nm UV light. c) TEM images of compound **1** prepared from THF/H$_2$O with 70% and 90% water. d) Emission spectra of compound **1** in PMMA (0.07 /100 mg) and in the solid powder with inserted photograph. e) Powder XRD pattern of solid powder **1** with the inset showing corresponding TEM image. f) GiWAXS spectrum of solid state **1** prepared from DCM. g) Powder XRD pattern and non-emissive photograph of solid powder **4**. h) Optimized geometrical conformation of **1**-dimer and **4**-dimer.

In order to compare the photophysical properties of these molecules in aggregated state, we investigated their emission spectra in THF/H$_2$O solution with different water fractions. Compounds **1**-**3** show similar emission behavior with gradual reduction of emission intensity when the water fraction changes from 0% to 50% (Figures 4a and S3). When the water fraction reaches 50%, their emission band starts to shift bathochromically and the reduction of emission intensity becomes slower. The maximum emission wavelength continues to shift into the green spectral region upon the water fraction increase from 70% to 90%, whereas the emission intensity keeps unchanged. Correspondingly, their solution luminescence colors are also clearly distinguished under UV light (Figure 4b).

To our surprise, the emission intensity of compound **1** in THF/H$_2$O with 90% water becomes even stronger than that with 70% water. Similarly, compounds **2** and **3** also exhibit relatively strong emission in THF/H$_2$O with 90% water. In addition, their absorbance (Figure S4) is blue shifted in THF/H$_2$O with 90% water as compared to that in THF, suggesting that these molecules form unique aggregates. As amorphous aggregates are normally present in high water content solution,[15,23,24] transmission electron microscopy (TEM) images show that these samples prepared from THF/H$_2$O with 70% water give irregular block aggregates. Interestingly, these aggregates turn regular in THF/H$_2$O with 90% water (Figure 4c). No major diffraction peaks observed in powder X-ray diffraction (Figure S5) suggests amorphous nature of **1** in THF/H$_2$O with 90% water. Its QY in THF/H$_2$O with 90% water is 40.3 %, indicating that it is very bright among the related amorphous materials.[23] These results demonstrate that this compound has strong emission both in dilute solution and amorphous aggregated state, unlike most of the traditional AIE molecules only showing bright emission from the crystal state.[15,23] Higher emission in solution as compared to that in amorphous aggregated state may be explained by the reduced molecular planarity in a loosely stacked state that cannot well restrict the molecule movement. Compounds **2** and **3** present relatively lower brightness than **1** in THF/H$_2$O with 90% water. For compound **4**, the decrease of emission intensity was observed with the increase of water fraction until complete quenching (Figure S6), well indicating that long alkyl chains could prevent unfavorable π-π stacking to maintain the emission pathway.

To further explore the photophysical properties upon the formation of the aggregated state, solid powders were prepared from selected solvent conditions. Solid powers **1**-**3** could be straightforwardly obtained from corresponding DCM solutions. All these powers display remarkably strong green emission with similar emission maximum around 500 nm (Figures 4d and S7). The redshifted emission as compared to the monomer one in THF (Figure 1b) or poly(methyl methacrylate) (PMMA, Figure 4d) is due to the formation of the excimer, proven by the broad fluorescence band without a vibrational structure in the solid state and a wavelength shift around 50 nm.[25] In addition, the redshifted UV spectra further confirm the formation of the excimer (Figure S7a). The QY of powder **1** is as high as 60.7%, followed by moderate QY of 36.3% for **2** and 26.7% for **3**. Compound **4** did not show any solid state emission, supporting that the alkyl chains have a positive influence on the solid state emission of this type of compounds.

To better understand the solid state emission mechanism, the solid state stacking was investigated by powder X-ray diffraction (XRD). It is known that the π-π stacking can often deteriorate the emission of molecules in the solid state with the *d* spacing around 3.5 Å through easily formed closed excimer or other species to facilitate non-radiative pathway.[20] The powder XRD pattern of **1** shows a weak peak at $2\theta = 25.1°$ with the *d* spacing of 3.5 Å (Figure 4e), indicating that the molecule only has a little π−π stacking in the solid state that would reduce the non-radiative decay of the excimer. On the contrary, strong powder XRD peaks below 10° reflect that the molecule basically adopts long distance stacking, featuring a crystalline nature in the solid state, which is also supported by regular block morphology in TEM image (Figure 4e). Such a crystalline effect would naturally enhance the emission *via* the reduction of molecular vibration and rotation. This is the reason why the emission of powder **1** is stronger than the emission of its amorphous aggregates. To further discern the stacking mechanism of powder **1**, we applied grazing incidence wide angle X-ray scattering (GiWAXS, Figure 4f) to characterize the packing orientation and *d* spacing. The in-plane (010) diffraction near $q^z = 1.5$ Å^{-1} corresponding to the π-π stacking distance of the solid[26] is very weak. Meanwhile, strong intermolecular interactions in q^{xy} direction verify that the distorted CS structure could restrict the molecular vibration and rotation, thereby improving the radiation transition process of excited state electrons.

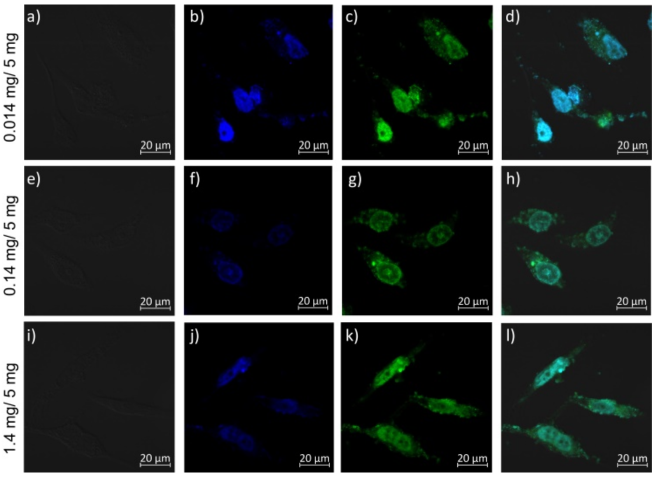

Figure 5. Confocal images of HepG2 cancer cells incubated with **1** (0.014 mg) / F127 (5 mg) for 6h: a) bright field, b) with 4',6-diamidino-2-phenylindole (DAPI) staining, c) with **1** staining, d) merged image of b) and c). Incubated with **1** (0.14 mg) / F127 (5 mg) for 6h: e) bright field, f) with DAPI staining, g) with **1** staining, and h) merged image of f) and g). Incubated with **1** (1.4 mg) / F127 (5 mg) for 6h: i) bright field, j) with DAPI staining, k) with **1** staining, and l) merged image of j) and k).

Compound **2** shows moderate intensity of the π-π stacking signal in the powder XRD pattern (Figure S8), suggesting its lower effectiveness of preventing the stacking through its linear side chains as compared with branched alkyl chains from compound **1**. In contrast, these signals in the powder XRD pattern of **4** are quite strong (Figure 4g), explaining its obvious emission quenching in the solid state. According to the optimized dimeric structures (Figure 4h) of **1** and **4** (**1**-dimer and **4**-dimer) by time-dependent DFT calculations, misaligned stacking was observed between two nearest benzene rings in **1**-dimer, whereas obvious face-to-face π-π stacking was shown in **4**-dimer. In addition, **1**-dimer presents strong absorption ($f = 2.8195$), corresponding to a dominant transition from HOMO to LUMO (Figure S9). However, such phenomenon is replaced by a main transition contribution from HOMO to LUMO-1 upon the photoexcitation in **4**-dimer. Corresponding oscillator strength of **4**-dimer is only 0.0063, originated from dark state of the solid form on account of strong π-π stacking interaction.

ACQ molecules normally need low concentrations to avoid aggregation for bioimaging,[27] whereas AIE molecules require high concentrations to form nano-aggregates for bioimaging.[28-30] These facts increase the preparation complicacy during the pretreatment, and would easily cause erroneous signal reading due to the fluctuation of probe concentration. Herein, we established a multiple live-cell imaging strategy by using compound **1** on account of its high brightness no matter in monomeric, amorphous or crystalline states. For meeting the practical use, we complexed 1.4 mg, 0.14 mg and 0.014 mg of **1** with amphiphilic triblock copolymer F127 of the same weight (5 mg) to obtain well-dispersed nanoparticles with an average diameter of around 200 nm in aqueous media (Figure S10). The viability of HepG2 cells (liver hepatocellular cells) is over 85% after the incubation with all three types of nanoparticles for 24 h (Figure S11), indicating that they are low toxic and suitable for bioimaging. Figure 5 shows confocal images of living HepG2 cells incubated with these nanoparticles for 6 h. The distribution throughout the cytoplasmic area of cells exhibits that these nanoparticles are successfully internalized by the cells. Three types of nanoparticles with different concentrations reveal bright emission in the green channel, demonstrating that compound **1** could efficiently image cells regardless of its low or high concentration.

In summary, we have developed a practical molecular engineering strategy by combining planar and distorted structures with long alkyl side chains to obtain DAπAD molecules with bright emission in dilute solution, amorphous state and solid crystalline state. The DPDA core and CT effect from D-A components allow the molecules to possess planar excited state with high emission in dilute solution. In addition, the distorted CS structures jointed with long alkyl chains could restrict molecular rotation and vibration in the solid state, enabling the strong emission. Weak π-π stacking of the compounds proven by powder XRD, GiWAXS and computational simulations is responsible for avoiding the non-radiative decay of the excimer to present strong emission. Efficient bioimaging in HepG2 cells has been achieved after the incubation with different concentrations of the probe. We believe that this strategy could be valuable for guiding the development of highly emissive molecules and materials in different situations, benefiting to their practical applications.

Acknowledgements

The research is supported by the Singapore Agency for Science, Technology and Research (A*STAR) AME IRG grant (A1883c0005), the Singapore National Research Foundation Investigatorship (NRF-NRFI2018-03), and partially by the National Key Research and Development Program of China (2017YFA0207700).

Keywords: bioimaging • luminescence• molecular engineering • molecular stacking • noncovalent interactions

[1] a) J. Qian, B. Z. Tang, *Chem.* **2017**, 3, 56. b) C. X. Yin, K. M. Xiong, F. J. Huo, J. C. Salamanca, R. M. Strongin, *Angew. Chem. Int. Ed*. **2017**, 56, 13188.
[2] a) X. Tan, T. Constantin, K. L. Sloane, A. S. Waggoner, M. P. Bruchez, B. A. Armitage, *J. Am. Chem. Soc*. **2017**, 139, 9001. b) X. Bai, Y. Huang, M. Lu, D. Yang, *Angew. Chem. Int. Ed*. **2017**, 129, 13053.
[3] a) L. Zhu, X. Li, Q. Zhang, X. Ma, M. Li, H. Zhang, Z. Luo, H. Ågren, Y. L. Zhao, *J. Am. Chem. Soc*. **2013**, 135, 5175; b) Y. Zhou, Y. Zhuang, X. Li, H. Ågren, L. Yu, J. Ding, L. Zhu, *Chem. Eur. J*. **2017**, 23, 7642.
[4] a) P. Xing, Y. Zhao, *Adv. Mater*. **2016**, 28, 7304. b) Y. Cheng, Y. Chang, Y. Feng, H. Jian, Z. Tang, H. Zhang, *Angew. Chem. Int. Ed*. **2018**, 57, 246.
[5] a) X. Chen, W. Zhang, *Chem. Soc. Rev*. **2017**, 46, 734. b) T. Senthilkumar, L. Zhou, Q. Gu, L. Liu, F. Lv, S. Wang, *Angew. Chem. Int. Ed*. **2018**, 57, 13114. c) F. Zhang, Q. Ni, O. Jacobson, S. Cheng, A. Liao, Z. Wang, G. Niu, *Angew. Chem. Int. Ed*. **2018**, 57, 7066.
[6] a) Z. Cheng, H. Shi, H. Ma, L. Bian, Q. Wu, L. Gu, S. Cai, X. Wang, W. Xiong, Z. An, W. Huang, *Angew. Chem. Int. Ed*. **2018**, 57, 678. b) Q. Zhang, D. Li, X. Li, P. White, J. Mecinovic, X. Ma, H. Ågren, R. Nolte, H. Tian, *J. Am. Chem. Soc.* **2016**, 138, 13541. c) S. Nishizawa, Y. Kato, N. Teramae, *J. Am. Chem. Soc.* **1999**, 121, 9463.
[7] a) K. T. Ly, R. W. Chen, H. W. Lin, Y. J. Shiau, S. H. Liu, P. T. Chou, Y. Chi, *Nat. Photon*. **2017**, 11, 63. b) L. S. Cui, H. Nomura, Y. Geng, J. U. Kim, H. Nakanotani, C. Adachi, *Angew. Chem. Int. Ed.* **2017**, 56, 1571.
[8] G. J. Li, T. Fleetham, J. Li, *Adv. Mater*. **2014**, 26, 2931.
[9] Z. Q. Xie, B. Yang, F. Li, G. Cheng, L. L. Liu, G. D. Yang, H. Xu, L. Ye, M. Hanif, S. Y. Liu, D. G. Ma, Y. G. Ma, *J. Am. Chem. Soc.* **2005**, 127, 14152.
[10] a) B. Geffroy, P. Le Roy, C. Prat, *Polym. Int*. **2006**, 55, 572; b) H. Wu, W. Chi, G. Baryshnikov, B. Wu, Y. Gong, D. Zheng, X. Li, Y. Zhao, X. Liu, H. Agren, L. Zhu, *Angew. Chem. Int. Ed*. **2019**, *58*, 4328.
[11] Y. Liu, Z. Zhou, L. Qu, B. Zou, Z. Chen, Y. Zhang, J. Xu, *Mater. Chem. Front*. **2017**, 1, 326.
[12] M. Belletête, J. Bouchard, M. Leclerc, G. Durocher, *Macromolecules* **2005**, 38, 880.
[13] J. Luo, Z. Xie, L. Cheng, H. Chen, C. Qiu, H. S. Kwok, X. Zhan, Y. Liu, D. B. Zhu, B. Z. Tang, *Chem. Commun*. **2001**, 37, 1740.
[14] a) B. K. An, D. S. Lee, J. S. Lee, Y. S. Park, H. S. Song, S. Y. Park, *J. Am. Chem. Soc*. **2004**, 126, 10232. b) H. Wu, Y. Zhou, L. Yin, C. Hang, X. Li, H. Ågren, L. Zhu, *J. Am. Chem. Soc*. **2017**, 139, 785-791.
[15] a) H. Wei, Z. Zhao, C. Wei, G. Yu, Z. Liu, B. Zhang, Z. Bian, C. Huang, *Adv. Funct. Mater*. **2016**, 26, 2085. b) S. A. Fateminia, Z. Wang, C. C. Goh, P. N. Manghnani, W. Wu, D. Mao, B. Liu, *Adv. Mater*. **2017**, 29, 1604100.
[16] G. Chen, W. Li, T. Zhou, Q. Peng, D. Zhai, H. Li, W. Z. Yuan, Y. M. Zhang, B. Z Tang, *Adv. Mater*. **2015**, 27, 4496.
[17] X. Yan, T. Cook, P. Wang, F. Huang, P. J. Stang, *Nat. Chem.* **2015**, 7, 342.
[18] a) Z. Zhang, C. L. Chen, Y. A. Chen, Y. C. Wei, J. Su, H. Tian, P. T. Chou. *Angew. Chem. Int. Ed*. **2018**, 130, 10028. b) S. Zhang, A. Qin, J. Sun, B. Tang, *Prog. Chem*. **2011**, 23, 623. c) W. Chen, C. L. Chen, Z. Zhang, Y. A. Chen, W. C. Chao, J. Su, H. Tian, P. T. Chou. *J. Am. Chem. Soc*. **2017**, 139, 1636.
[19] a) L. Zhu, H. Tran, F. L. Beyer, S. D. Walck, X. Li, H. Ågren, L. M. Campos, *J. Am. Chem. Soc*. **2014**, 136, 13381. b) L. Zhu, M. T. Trinh, L. Yin, Z. Zhang. *Chem. Sci*. **2016**, 7, 2058.
[20] L. Zong, Y. Xie, C. Wang, J. R. Li, Q. Li, Z. Li, *Chem. Commun*. **2016**, 52, 11496.
[21] H. G. Lu, Y. Zheng, X. W. Zhao, L. J. Wang, S. Q. Ma, X. Q. Han, B. Xu, W. J. Tian, H. Gao, *Angew. Chem. Int. Ed*. **2016**, 55, 155.
[22] Z. Zhao, S. Chen, J. W. Lam, P. Lu, Y. Zhong, K. S. Wong, H. S. Kwok, B. Z. Tang, *Chem. Commun*. **2010**, *46*, 2221.
[23] a) D. Ding, K. Li, B. Liu, B. Z. Tang, *Acc. Chem. Res*. **2013**, 46, 2441. b) Z. Zhang, B. Xu, J. Su, L. Shen, Y. Xie, H. Tian, *Angew. Chem. Int. Ed*. **2011**, 50, 11654. b) Z. An, C. Zheng, Y. Tao, R. Chen, H. Shi, T. Chen, Z. Wang, H. Li, R. Deng, X. Liu, W. Huang, *Nat. Mater*. **2015**, 14, 685.
[24] Z. Zhao, B. Chen, J. Geng, Z. Chang, L. Aparicio-Ixta, H. Nie, C. C. Goh, L. G. Ng, A. Qin, G. Ramos-Ortiz, B. Liu, B. Z. Tang, *Part. Part. Syst. Charact*. **2014**, 31, 481.
[25] H. Ohkita, S. Ito, M. Yamamoto, Y. Tohda, K. Tani, *J. Phys. Chem. A* **2002**, *106*, 2140.
[26] Q. V. Hoang, C. E. Song, S. J. Moon, S. K. Lee, J. C. Lee, B. J. Kim, W. S. Shin, *Macromolecules* **2015**, 48, 3918.
[27] G. Battistelli, A. Cantelli, G. Guidetti, J. Manzi, M. Montalti, *Nanobiotechnology* **2016**, 8, 139.
[28] L. Yan, Y. Zhang, B. Xu, W. Tian, *Nanoscale* **2016**, 8, 2471.
[29] W. C. Wu, C. Y. Chen, Y. Tian, S. H. Jang, Y. Hong, Y. Liu, W. C. Chen, *Adv. Funct. Mater*. **2010**, 20, 1413.
[30] D. Li, W. Qin, B. Xu, J. Qian, B. Z. Tang, *Adv. Mater*. **2017**, 29, 1703643.

Entry for the Table of Contents (Please choose one layout)

Layout 1:

COMMUNICATION

The integration of planar and distorted structures with long alkyl side chains to obtain molecules with high emission efficiency both in solution and the solid state is demonstrated. Efficient intracellular bioimaging using the molecules with different concentrations demonstrates the possibility of applying the highly emissive systems.

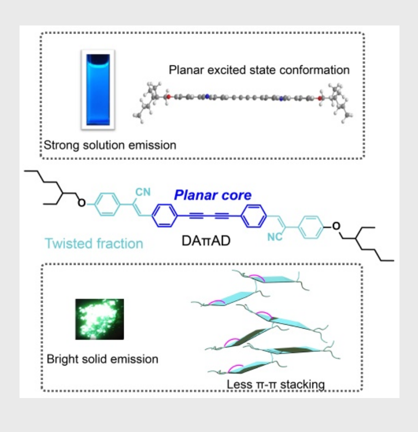

Hongwei Wu, Zhao Chen, Weijie Chi, Bindra Anivind Kaur, Long Gu, Cheng Qian, Bing Wu, Bingbing Yue, Guofeng Liu, Guangbao Yang Liangliang Zhu, Yanli Zhao**

Page No. – Page No.

Structural Engineering of Luminogens with High Emission Efficiency both in Solution and the Solid State